Table S.1. AlphaFold IDs, UniProt accessions, and average pLDDT (Predicted Local Distance Difference Test) scores of target proteins analyzed in relation to LSD1 inhibitor RG6016.

AlphaFold ID	Protein	UniProt	Average pLDDT
AF-P19075-F1-v4	TSPAN8	P19075	88.12 (High)
AF-Q9HBH7-F1-v4	BEX1	Q9HBH7	66.95 (Low)
AF-Q00994-F1-v4	BEX3	Q00994	64.32 (Low)
AF-P01258-F1-v4	CALCA	P01258	64.56 (Low)
AF-P14209-F1-v4	CD99	P14209	60.72 (Low)
AF-Q9BZI1-F1-v4	IRX2	Q9BZI1	54.11 (Low)
AF-Q96JG8-F1-v4	MAGED4	Q96JG8	53.72 (Low)
AF-Q99784-F1-v4	OLFM1	Q99784	79.39 (High)
AF-Q9BYH1-F1-v4	SEZ6L	Q9BYH1	68.48 (Low)
AF-Q07654-F1-v4	TFF3	Q07654	80.13 (High)
AF-Q08629-F1-v4	SPOCK1	Q08629	64.56 (Low)

Table S.2. Molecular docking data of RG6016 (ORY-1001) with 14 analyzed proteins. This table lists the docking results for all 14 proteins analyzed with RG6016, including binding energies, hydrogen bond interactions, and additional interaction details where applicable.

Protein	Docking Score (Kcal/mol)	Aminoacid Interaction	Hydrogen Bond Distance (Å)	Number of conventional hydrogen bonds
LSD1/FAD complex	-7.2	ASP555	2,21	3
		ASN806	2,57	
		ASN806	2,60	
TSPAN8	-7.4	ASN16	2,44	2
		ASN16	2,48	
UCHL1	-7.2	MET124	2,54	1
MYC	-7.0	ALA280	2,63	2
		ALA280	2,79	
BEX1	-4.9	MET67	2,28	1
BEX3	-4.4	TRP49	3,02	1
CALCA	-5.0	PHE3	2,05	1
CD99	-5.2	–	–	–

IRX2	-6.3	–	–	–
MAGED4	-6.7	LYS427	2,60	2
		PRO433	2,29	
OLFM1	-6.6	ASP360	2,86	5
		ASP360	2,95	
		GLU361	2,28	
		PRO456	2,44	
		PRO456	2,72	
SEZL6	-6.0	–	–	–
TFF3	-6.2	TYR58	2,29	1
SPOCK1	-6.2	CYS304	2,20	2
		SER208	1,86	

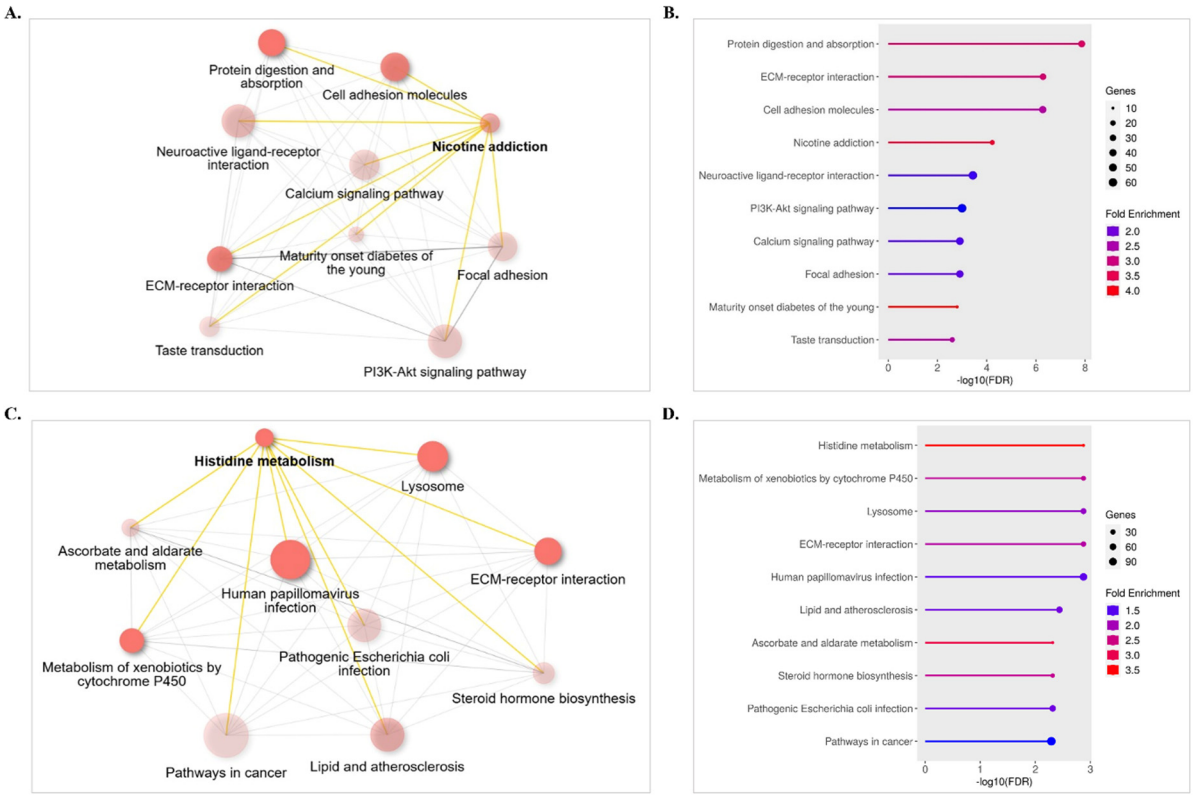


Figure S.1. Pathway enrichment analysis of DEGs in RG6016-treated PDX samples. **(A)** Network graph of downregulated pathways visualizing genetic connections among pathways. Node size represents relative importance of each pathway, while edges indicate shared genes between pathways. **(B)** Bar plot of top 10 downregulated pathways ranked by $-\log_{10}$(FDR) values. Colors represent fold enrichment levels. **(C)** Network graph of upregulated pathways illustrating relationships among biological processes activated following RG6016 treatment. **(D)** Bar plot of top 10 upregulated pathways ranked by $-\log_{10}$(FDR) values and color-coded based on fold enrichment.

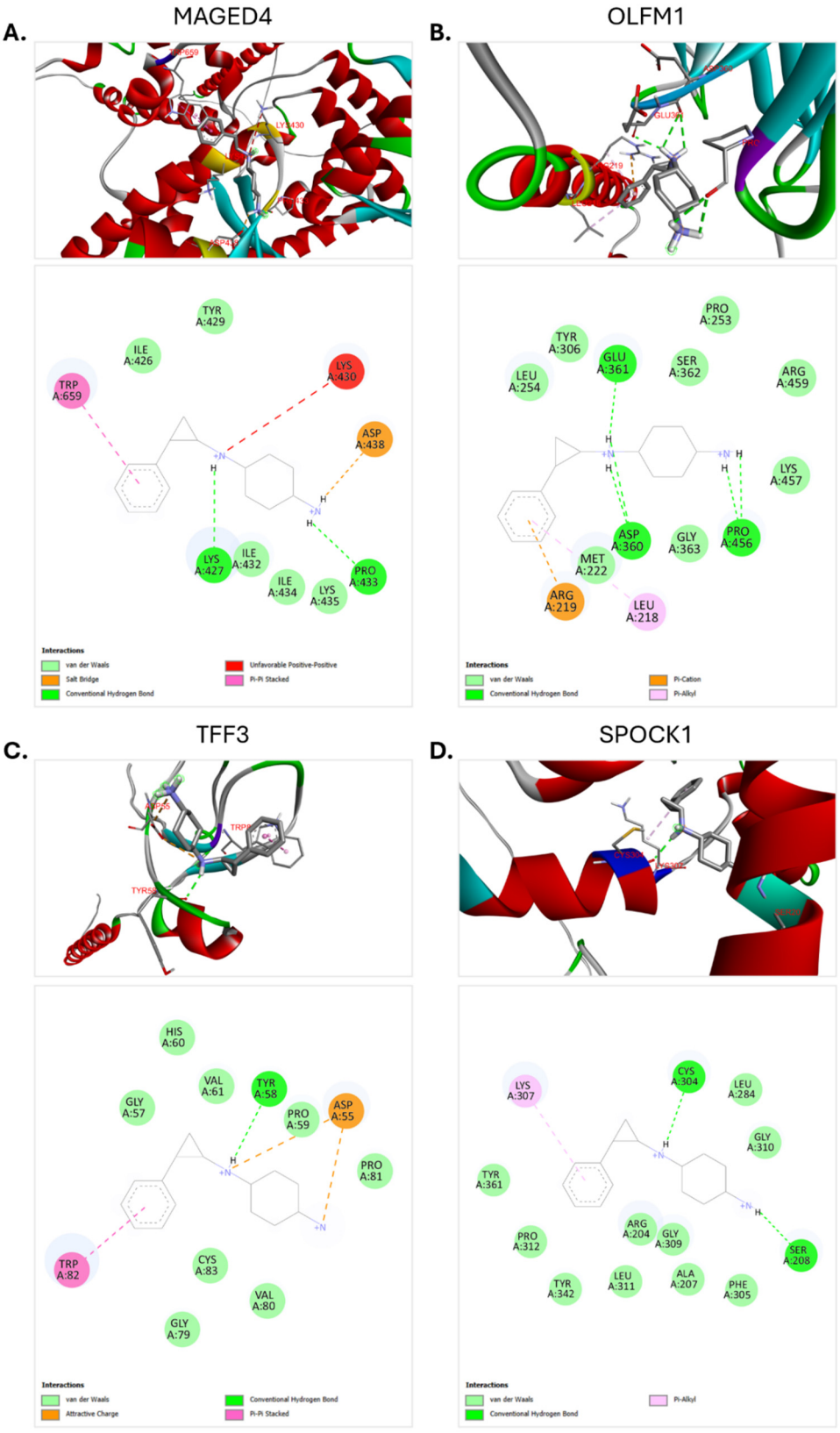


Figure S.2. A visualization of the molecular docking interactions between RG6016 (ORY-1001) and MAGED4 **(A)**, OLFM1 **(B)**, TFF3 **(C)**, and SPOCK1 **(D)** proteins. The upper panel shows the three-dimensional binding poses of RG6016 within each protein's active site, while the lower panel displays two-dimensional interaction diagrams, including hydrogen bonds, hydrophobic interactions, salt bridges, and other complementary binding interactions.

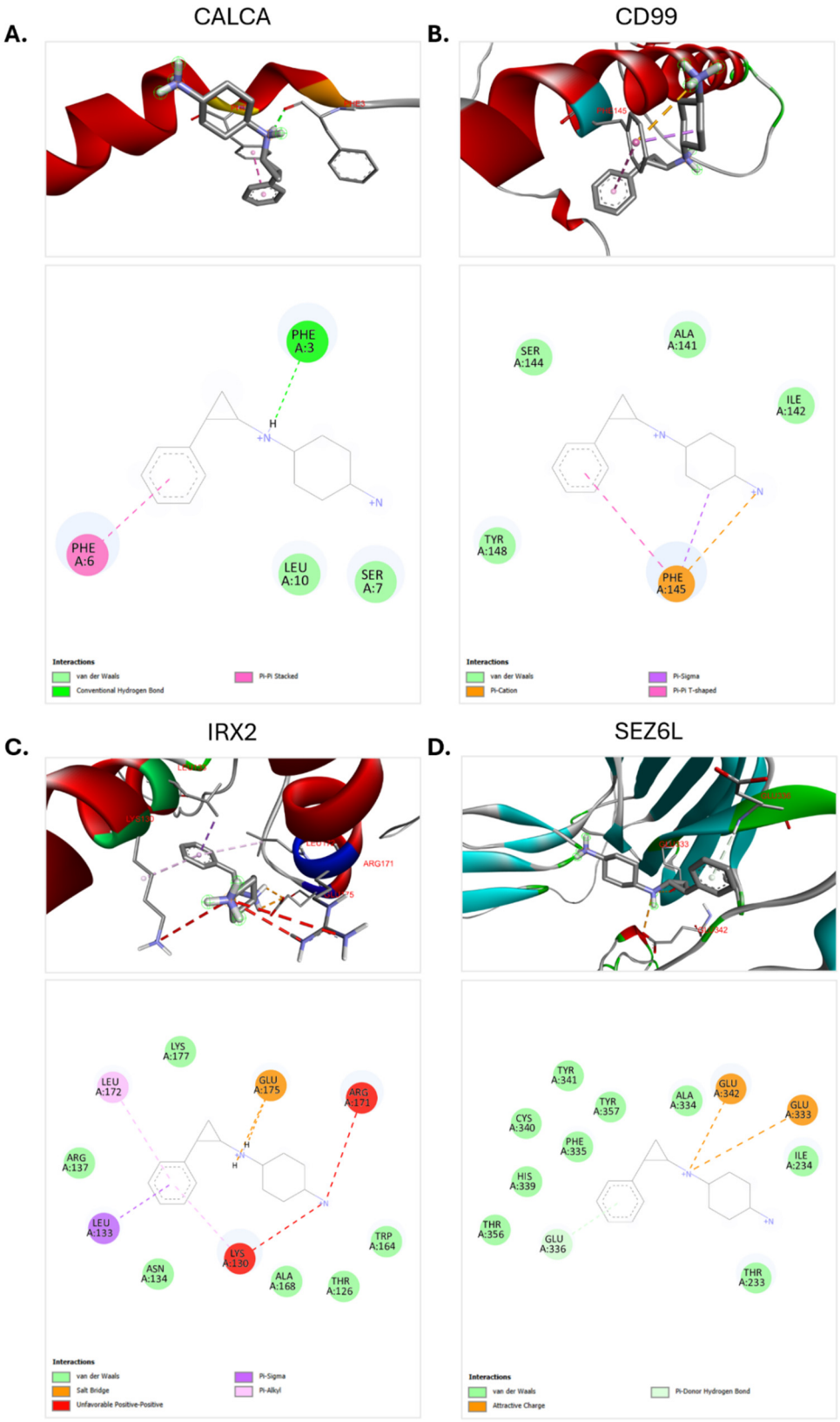


Figure S.3. A visualization of the molecular docking interactions between RG6016 (ORY-1001) and CALCA **(A)**, CD99 **(B)**, IRX2 **(C)**, and SEZ6L **(D)** proteins. The upper panel displays the three-dimensional binding poses of RG6016 within the binding sites of each protein. The lower panel presents two-dimensional interaction diagrams, illustrating hydrogen bonds, hydrophobic interactions, π interactions, and other complementary binding types.

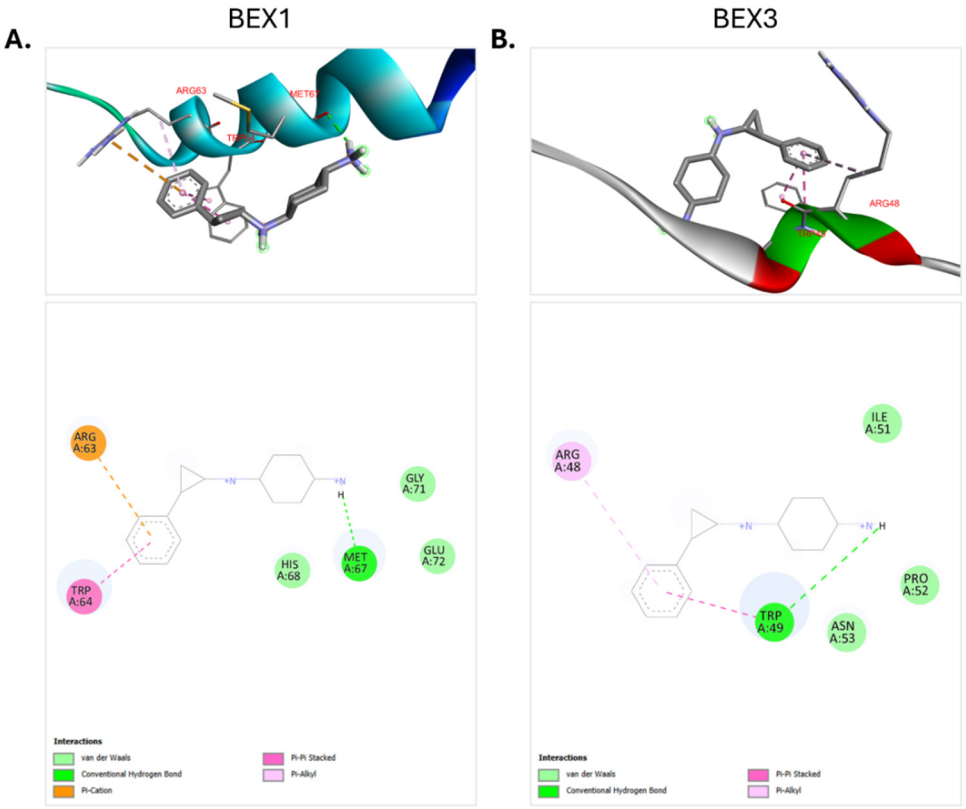


Figure S.4. A visualization of the molecular docking interactions between RG6016 (ORY-1001) and BEX1 **(A)** and BEX3 **(B)** proteins. The upper panel shows the three-dimensional binding positions, while the lower panel presents two-dimensional interaction maps including hydrogen bonds, π interactions, and van der Waals interactions.